Australian Government
Department of Defence
Defence Science and
Technology Organisation

Examples of a Class of Chaotic Radar Signals

Graham V. Weinberg and Aris Alexopoulos

Electronic Warfare and Radar Division
Defence Science and Technology Organisation

DSTO–TN–0660

ABSTRACT

This note is a preliminary study of radar signals viewed as discretised nonlinear dynamical systems. Motivated by [Haykin and Li 1995], a class of recursively defined signals is introduced, and two specific examples are considered. It will be shown that such signals can exhibit complex dynamics in phase space. This means that they experience sensitive dependence on initial conditions. Using the Lyapunov spectrum, we determine the stability of these signals. We will also investigate whether such signals are of practical use in radar by examining their ambiguity functions.

Published by

Defence Science and Technology Organisation
PO Box 1500
Edinburgh, South Australia, Australia 5111

Telephone: (08) 8259 5555
Facsimile: (08) 8259 6567

AR No. AR-013-488
August, 2005

APPROVED FOR PUBLIC RELEASE

Examples of a Class of Chaotic Radar Signals

EXECUTIVE SUMMARY

This work is a preliminary investigation of a class of radar signals generated by recursively defined functions. Signals are of fundamental importance in radar, since a radar system uses transmitted and returned signals from the environment to decide on the presence of targets, as well as their range, bearing and speed. The issue of an appropriate choice of signal is complex, and application dependent. There are many types of signals, including linear frequency modulation, single frequency pulse trains, step frequency pulse trains, step frequency continuous waves, pseudorandom codes and random noise. This note is a brief examination of a new class of signals, known as chaotic signals. Such signals may be of importance in radar for a number of reasons. The first is that they are generated from a deterministic map, but can be made to appear as noise. This would be useful from an electronic protection point of view. Secondly, since these signals can be generated from a single dynamical system, with different control parameters and initial conditions, it may be possible to reduce the need for a comprehensive library of signals in a radar system.

The generation of such signals, as a discrete time dynamical system, will be outlined. We investigate the stability of such signals, using the Lyapunov spectrum. Two such signals will be examined, generated from recursions of sinusoidal functions. The first is generated by recursions of the function $\psi(x, \lambda) = \lambda \sin(2\pi x)$, while the second is generated via $\psi(x, \lambda) = \sin(2\pi x) + \cos(2\pi\lambda x)$. We will show signals generated from these functions have sensitive dependence on initial conditions, and a very interesting phase portrait. The radar ambiguity function is used to decide whether these signals are of practical use in radar.

Authors

Graham V. Weinberg
Electronic Warfare and Radar Division

Graham V. Weinberg is a research scientist, working in the general area of radar signal processing, and specifically, in radar detection theory. He is a specialist in mathematical analysis and applied probability, and holds a Doctor of Philosophy Degree from The University of Melbourne, in stochastic processes.

Aris Alexopoulos
Electronic Warfare and Radar Division

Aris Alexopoulos is a theoretical physicist and holds first class Honours and PhD degrees. At DSTO his work interests are in the areas of phased array radar, electromagnetic propagation, non-linear and fractal electrodynamics and quantum technology for military applications.

Contents

Figures

1 Introduction

The purpose of this note is to consider a class of recursively defined signals that exhibit complex dynamics in phase space. This work arose out of an interesting radar signal in [Haykin and Li 1995]. This signal exhibits sensitive dependence on initial conditions, and has an unusual self replicating feature in phase space. The main issue to be addressed in this note is whether such signals are of practical use in radar.

Signals are of paramount importance in radar. Radar systems use different types of signals for specific applications in varying situational contexts [Ringer, Frazer and Anderson 1999 and Lin and Liu 2004]. There are hence many different classes of radar signals. [Ringer, Frazer and Anderson 1999] describes four classes of radar signals, based upon their characteristics and ambiguity functions. Linear frequency modulation, single frequency pulse trains, step frequency pulse trains, step frequency continuous waves, pseudorandom codes and random noise are examples pointed out in [Lin and Liu 2004]. A relatively new class of signals are those which have chaotic dynamics [Lin and Liu 2004, Sobhy and Shehata 2000 and Wu *et. al.* 2001]. Such a class of signals exhibits a phenomenon known as *sensitive dependence on initial conditions*. These signals may be useful in radar in the way code division multiple access (CDMA) is useful in digital telephony [Zigangirov 2004]. The advantage of CDMA is that the transmitted signal appears as noise to all but the intended recipient. It is possible that chaotic signals could be used to mask the signal within environmental noise and interference, so that targets may not be aware of the presence of a scanning radar. Hence these signals may be of use as an electronic protection measure for the radar platform.

Chaos theory investigates strange behaviour found in nonlinear deterministic dynamical systems. Such unusual behaviour in dynamical systems was first discovered by Poincaré, in 1903, who was attempting to show rigorously that the solar system, as modelled by Newton's Laws of Motion, is dynamically stable [Strogatz 1994]. He discovered that small differences in initial conditions can produce drastically different final solutions. Another early important study of dynamical systems exhibiting strange behaviour is [Lorenz 1963], who developed a system of coupled nonlinear differential equations to model weather patterns, and also observed this strange sensitivity to initial conditions. Lorenz coined the phrase "the butterfly effect" to illustrate this sensitivity. The latter implies a butterfly flapping its wings in one part of the world can have an effect on the weather in another distant part of the world. The term *chaos* first appeared in a dynamical systems context in [Li and Yorke 1975].

A chaotic dynamical system is a nonlinear dynamical system whose output has sensitive dependence on initial conditions. Chaos theory is the analysis of the behaviour of such systems. As such, chaos theory is not really a theory of chaos, but is more concerned with understanding the complex behaviour of nonlinear dynamical systems. We will introduce briefly the study of such systems, and in particular, will be interested in determining under what conditions such a system becomes chaotic. A class of radar signals will be introduced. We will examine two signals in this class, and apply the ambiguity function to see whether they are of practical use in radar.

2 Radar Signals and Dynamical Systems

In this section we introduce a class of radar signals, defined through a dynamical system, and outline how such signals can be classified as chaotic. To this end, we introduce necessary definitions, as well as the three so-called *signatures of chaos*. Some useful references on dynamical systems and chaos are [Drazin 1992, Strogatz 1994, Hale and Koçak 1991, Haykin and Puthusserypady 1999 and Williams 1997]. References on radar signals include [Bird 1974, Cook and Bernfield 1967, Helstrom 1960, Levanon 1988 and Levanon and Mozeson 2004].

2.1 Signals as Dynamical Systems

Let $\mathcal{S}$ be the class of all real-valued radar signals, including both those defined on a discrete and continuous time domain. In order to motivate the work to follow, we consider a subclass of $\mathcal{S}$ that can be defined through a dynamical system. Assume $x(t) \in \mathcal{S}$, is continuous and differentiable within a domain. From a physical point of view, the derivative of this signal, $\frac{d}{dt}x(t)$, is the rate of change of it in a propagating medium. We may hence analyse the signal via this rate of change, so assume that $\phi(t) = \frac{d}{dt}x(t)$. In addition to this, we may assume that in some cases, $\phi(t)$ can be expressed as a nonlinear composition of the signal $x(t)$. Thus, there may exist a function ψ such that $\phi(t) = \psi(x(t))$. Hence, equivalently, $x'(t) = \psi(x(t))$.

To show this class of signals is nonempty, consider the signal $x(t) = \sin(t)$, for $t \in D = (0, \frac{\pi}{2})$. Its derivative is $x'(t) = \phi(t) = \cos(t)$. Choose $\psi(t) = \sqrt{1-t^2}$. Then $\psi(x(t)) = \phi(t)$ on D. Hence, we can define the class of signals $\mathcal{C} = \{x(t) : \text{there exists a } \psi : x'(t) = \psi(x(t))\}$.

As in [Haykin and Li 1995], we can consider discretised time, since signals are often digitised so they can be processed by digital computers. Hence we can further restrict attention to the subclass $\mathcal{C}_{\mathcal{D}} \subset \mathcal{S}$ defined by the set $\{x(n) : \text{there exists a } \psi : x(n+1) = \psi(x(n))\}$. The function ψ defined in the set $\mathcal{C}_{\mathcal{D}}$ will be referred to as a *generator* of a signal.

We specialise the discussion to one dimensional discrete maps, since we will be exclusively studying signals from the class $\mathcal{C}_{\mathcal{D}}$. A *dynamical system* is a physical system which is described by a deterministic set of rules that change with time. Suppose the variables $\{x(n) : n \in \mathbb{N}\}$ describe the states of the system at each discrete time point n. Then we assume there is a generator function ψ, defined on the range of $x(n)$, such that

$$x(n+1) = \psi(x(n)). \tag{1}$$

The generator ψ in (1) determines the evolution of the system, and in general will be nonlinear. We refer to the system's state space as the space $\mathcal{M}$ where the functions $x(n)$ take values. In the context of the discrete signals considered here, the state space will be subsets of the real line. As an example, the well-known *Logistic Map* has generator $\psi(x) = \lambda x(1-x)$, and the corresponding map, defined through (1) has initial value

$x(0) \in (0, 1)$. We will show that this map becomes unstable as λ changes, using its Lyapunov spectrum.

It is not difficult to write down the general solution to (1). Let $\psi^{(k)}(x)$ be the kth composition of ψ with itself. By a simple recursion, it is not difficult to show that

$$x(n) = \psi^{(n)}(x(0)) \tag{2}$$

is the solution to (1).

The path in the state space that a dynamical system, defined through (2), traces out is called its *trajectory or orbit.* A *dissipative dynamical system* is characterised by convergence of trajectories in its state space. An *attractor* is defined to be a set of points to which all neighbouring trajectories converge in phase space. The attractor set consists of all limit points of the discrete map defined by (1). A *point attractor* is a single point to which trajectories converge, also known as a *stable fixed point.* A dynamical system may have a set of points which are visited periodically. Such points are referred to as a *stable limit cycle, with periodic orbits.* An attractor is also an *invariant set*, meaning that when a trajectory starts in it, it remains in the set forever. The largest subset of an attractor set, consisting of the largest set of points to which all nearby orbits converge, is called the *basin of attraction.* In a nonlinear dynamical system, where orbits in an attractor move apart with increasing time, the system is said to possess a *strange attractor.* Such dynamical systems are referred to as being *chaotic.*

Chaos is often defined to be the aperiodic long run behaviour in a deterministic dynamical system that exhibits sensitive dependence on initial conditions. There are three so-called *signatures of chaos*:

1. *Aperiodicity* in limiting behaviour, meaning that the system does not converge to a single point as discrete time increases without bound;
2. It is a *deterministic* system, with no stochastic component, but is nonlinear;
3. The system exhibits *sensitive dependence on initial conditions*, meaning arbitrarily close trajectories will diverge apart exponentially fast.

2.2 Lyapunov Spectrum

Lyapunov exponents of a dynamical system provide a quantitative measure of its sensitivity to initial conditions. The *Lyapunov spectrum* of a map is a plot of its Lyapunov exponents. As pointed out in [Haykin and Li 1995], they give the average rate of convergence or divergence of the system along the principal axes in phase space. The existence of at least one positive Lyapunov exponent is a necessary condition for a dynamical system to be chaotic [Newhouse 1984]. Hence, given a dynamical system, if we can establish that there is at least one positive Lyapunov exponent, then we can be certain the system will exhibit chaotic dynamics.

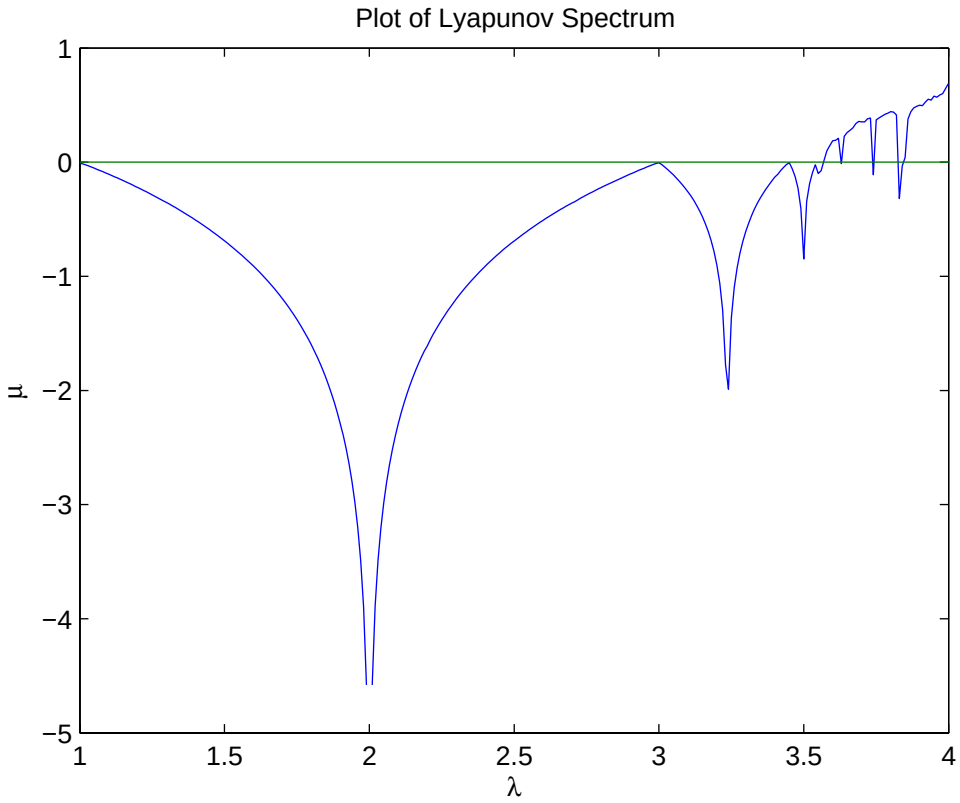

Figure 1: A plot of the Lyapunov spectrum for the logistic map $x(n+1) = \lambda x(n)(1-x(n))$, *with* $x(0) = 0.1$.

For a dynamical system, such as that generated by (1), where we know the generator ψ, it has been shown that the complete Lyapunov spectrum can be easily computed [Benettin *et. al.* 1980]. This can be done by considering the perturbation of a point of the system, and applying a linear stability analysis [Haykin and Li 1995].

We focus on the calculation of Lyapunov exponents in the current context of one-dimensional discrete maps. The ideas to follow can be found in [Williams 1997 and Wolf 1986]. Consider the dynamical system (1), with initial condition $x(0)$. Examine a small perturbation of this starting point, defined by $x(0) + \delta(0)$, where the initial separation $\delta(0)$ is assumed to be very small. Suppose $\delta(n)$ is the separation after n iterations of the system. If $|\delta(n)| \approx |\delta(0)|\, e^{n\mu}$, then μ is called a *Lyapunov exponent*. These can be found, for a trajectory starting at $x(0)$, from the limit

$$\mu = \lim_{m\to\infty} \left(\frac{1}{m} \sum_{j=1}^{m-1} \log \left| \psi'(x(j)) \right| \right). \tag{3}$$

Further details can be found in [Williams 1997]. It is clear from (3) that μ depends on the starting point $x(0)$. For a given attractor, μ is invariant in the basin of attraction [Drazin 1992]. If a Lyapunov exponent is negative for a particular orbit, then the orbit

either has a stable fixed point, or a stable limit cycle. In the case where it is positive, the orbit is in a strange attractor, and the trajectory will be chaotic. Figure 1 is a plot of the Lyapunov spectrum for the Logistic map introduced previously, with $x(0) = 0.1$. As can be observed, the map has stable dynamics until at approximately $\lambda = 3.6$, where it becomes chaotic, followed by periods of stability and then chaos.

In the current context of radar signals in the class $\mathcal{C}_{\mathcal{D}}$, we can calculate the Lyapunov spectrum, and use it to decide which parameter values generate a chaotic signal.

2.3 Radar Ambiguity Function

An important tool in the design and evaluation of radar signals is the *radar ambiguity function* [Bird 1974, Levanon 1988, Levanon and Mozeson 2004 and Ringer, Frazer and Anderson 1999]. As pointed out in [Levanon and Mozeson 2004], it represents the time response of a signal filter matched to a specified signal of finite energy, when the signal is received with a time delay τ and a Doppler shift ϕ relative to the nominal values expected by the filter. We denote this function as $\chi(\tau, \phi)$. There are a number of variations in the definition taken for $\chi(\tau, \phi)$. We base ours closely on that in [Levanon 1988 and Levanon and Mozeson 2004]. For a discretised complex-valued signal $x(n)$, of length N, the ambiguity function is defined to be

$$\chi(\tau, \phi) = \frac{1}{N} \sum_{n=1}^{N} x(n) x^*(n + \tau) e^{-i\phi n}, \tag{4}$$

where the star denotes complex conjugate.

[Ringer, Frazer and Anderson 1999] contains a detailed discussion of the desirable features of radar ambiguity functions. The following discussion is based closely on this source. One perspective in the radar community is that an ideal radar signal is one which produces an ambiguity function that is a spike at the origin, and zero everywhere else. The reason for this is that it can be shown in order to optimally detect a target, it is necessary to maximise $\chi(0, 0)$. Additionally, in order to minimise the probability of false detections of targets, it is necessary to minimise $\chi(\tau, \phi)$ with $(\tau, \phi) \neq (0, 0)$.

As pointed out in [Levanon 1988], the ambiguity function was not introduced to radar signal analysis via the matched filter, but as a normed difference between a signal and a copy of it that differs in time delay and Doppler shift [see Bird 1974]. To illustrate this, suppose we have a discrete radar signal $x(n)$, which we assume is a member of the Hilbert space of complex valued signals of finite energy, discrete time modulo N, with inner product $< x_1, x_2 >= \sum_{j=0}^{N} x_1(j) x_2^*(j)$. The norm induced by this inner product is $||x|| = \sqrt{< x, x >}$. We can consider the return from a radar signal x as a time delay and Doppler shifted version of the original, and so define an operator $D(\tau, \phi)x(j) = e^{2\pi i \phi j/N} x(j + \tau)$. By applying properties of inner products, it can be shown that

$$||x - D(\tau, \phi)x||^2 = 2||x||^2 - 2\mathbf{Re}\left(\chi(\tau, \phi)\right), \tag{5}$$

where **Re** is the real part of a complex number. Expression (5) is the squared normed difference between the original signal x and its time delayed and Doppler shifted version

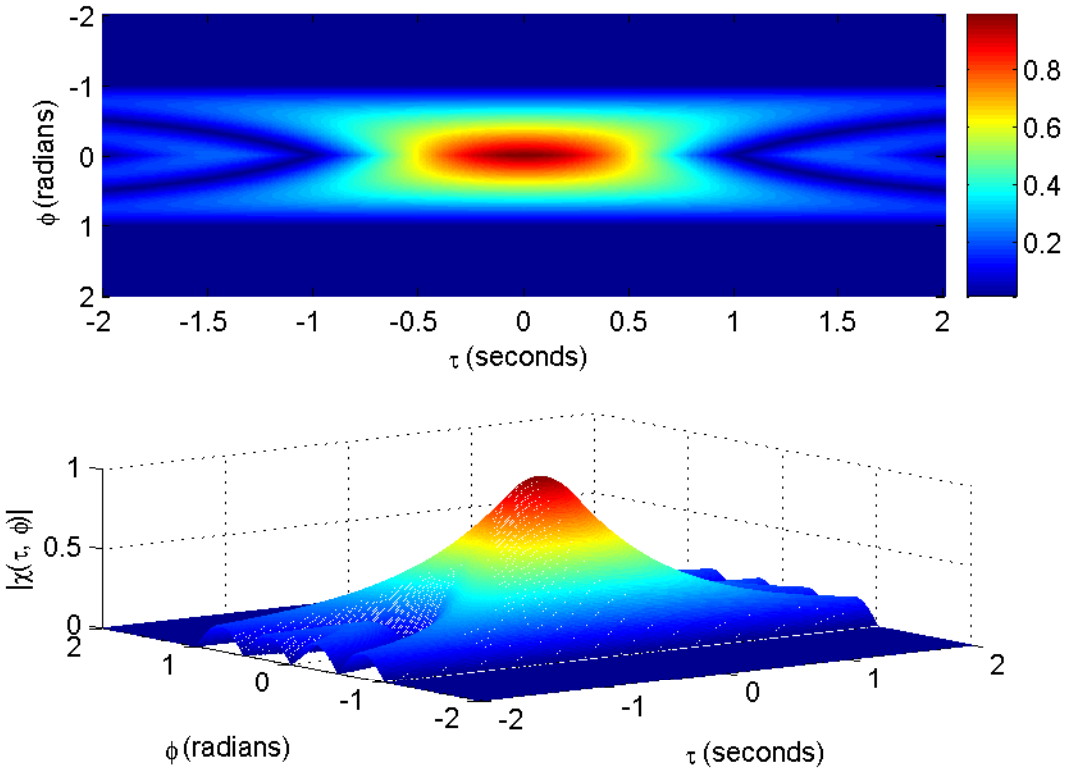

Figure 2: Ambiguity function plots for a single frequency pulse. The delay unit (τ) is seconds, the Doppler unit (ϕ) is radians and the absolute value of the ambiguity function scale is linear. The pulse duration is 1 second.

$D(\tau, \phi)x$. To be able to differentiate between the two signals, we require the normed difference (5) to be maximised, except in the case where $\tau = \phi = 0$. In the latter case, the two signals are the same. Note that $||x||^2$, which is the signal energy, is constant for a given signal. Hence, to maximise (5), we need to minimise $\mathrm{Re}\,(\chi(\tau, \phi))$. This can be achieved if we minimise the absolute value of the ambiguity function (4). Hence, in order to optimally differentiate a signal from its time delay and Doppler shifted version, we need an ambiguity function that is like a "thumbtack", namely a spike at the origin and almost zero everywhere else.

It is, however, impossible to produce a radar signal with such an ambiguity function. The main reason for this is that it can be shown that the volume under $|\chi(\tau, \phi)|$ is a non-zero constant, whose square is the energy in the transmitted signal, and cannot be confined to a single spike at the origin.

If the absolute value of the ambiguity function has a large volume located near the origin, producing a wide peak, then the ability of the radar to resolve targets will be limited in that region. False detections may occur if there are large spikes in the ambiguity function's absolute value away from the origin. This may also cause the masking of secondary targets.

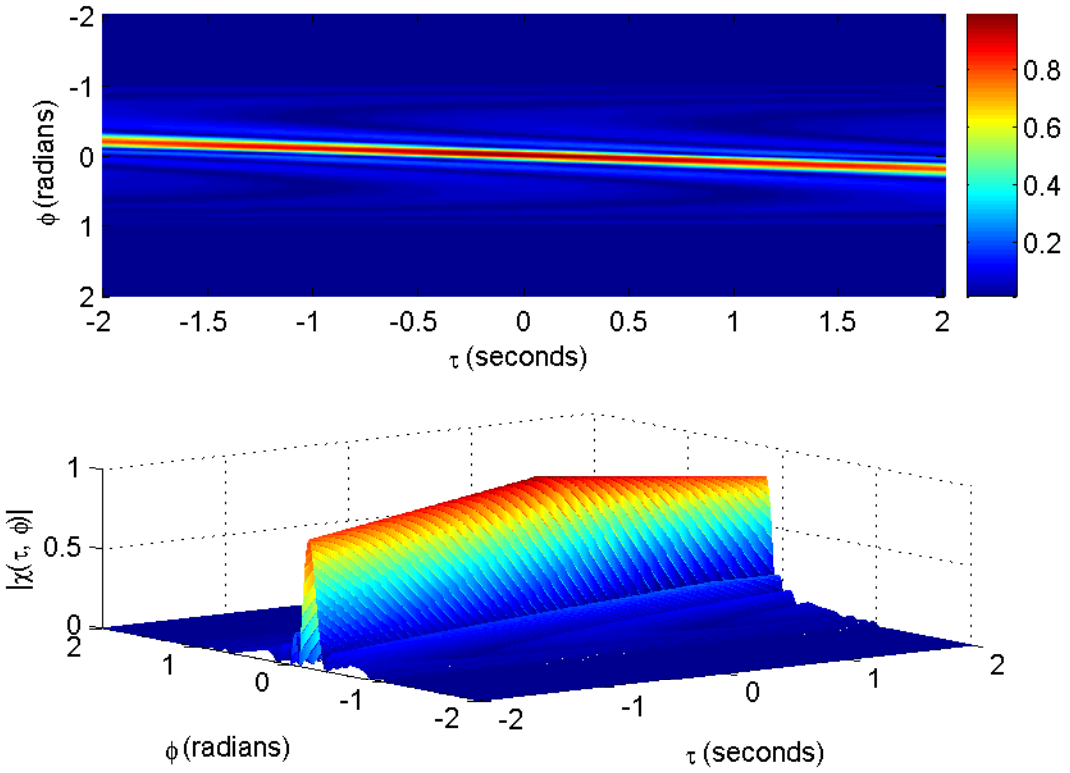

Figure 3: Ambiguity function plots for a linear FM pulse, with the same scale units as for Figure 2, including a linear scale for the absolute value of the ambiguity function. As for the example in Figure 2, the pulse duration is 1 second.

Figures 2 and 3 are plots of the absolute value of ambiguity functions of two standard radar signals. The plots in Figure 2 are for a standard single frequency pulse, while that for Figure 3 are for a standard linear FM pulse [see Levanon 1988 and Levanon and Mozeson 2004 for more details]. In each Figure, two subplots are used. The first one shows the ambiguity function as a coloured contour map, with colours illustrating the magnitude of the function at each time delay (τ) and Doppler level (ϕ). The second plot shows the ambiguity function as a surface in space. Both signals have a pulse duration of 1 second. The plots of Figure 2 show that the ambiguity function has a large ridge along the axis $\phi = 0$. As pointed out in [Ringer, Frazer and Anderson 1999], this means that the corresponding signal will provide high resolution in Doppler shift, but not in time delay. One signal design feature that can be deduced from the ambiguity function plot of Figure 2 is that a shorter pulse will provide better range resolution than a longer one. The ambiguity function plots in Figure 3 show a large ridge at an angle to the τ and ϕ axes. It is pointed out in [Ringer, Frazer and Anderson 1999] that the signals corresponding to such ambiguity functions will have some difficulty in resolving targets. Specifically, it is possible the signal will resolve all targets well, except those with a Doppler and time delay product which matches the angle of the ridge.

We will use the ambiguity function in the following section, to decide whether two examples of members of the class $\mathcal{C}_{\mathcal{D}}$ would be of potential applicability in a radar context.

3 Two Radar Signals with Chaotic Behaviour

This section introduces two signals from the class $\mathcal{C}_{\mathcal{D}}$, and investigates their behaviour.

3.1 Example 1: $\psi(x, \lambda) = \lambda \sin(2\pi x)$

The first signal is that with generator $\psi(x, \lambda) = \lambda \sin(2\pi x)$. To illustrate the sensitivity of the corresponding signal, defined through (2), to initial conditions, consider Figure 4. This is a plot of the differences of two versions of (2). We denote these two signals as $x(n)$ and $y(n)$ respectively. One has initial value $x(0) = 2$, while the second starts with $y(0) = 2 + 10^{-12}$. In both cases, $\lambda = 2$. The plots in Figure 4 show the original signal $x(n)$, the perturbed signal $y(n)$ and their pointwise differences $x(n) - y(n)$. It would not be unreasonable to assume that these signals would evolve almost identically, given the difference in initial values is 10^{-12}. Figure 4 shows that they do initially, but there is then a divergence apart. As pointed out previously, such behaviour is characteristic of a chaotic system.

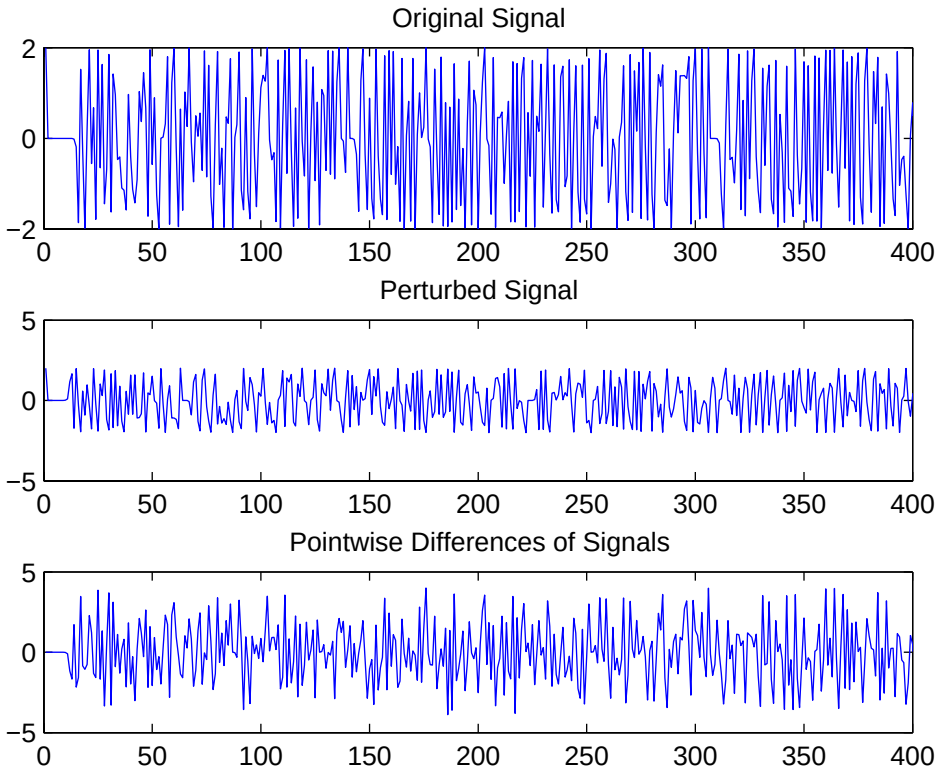

Figure 4: Plots of signals with generator $\psi(x, \lambda) = \lambda \sin(2\pi x)$. The first plot shows an orbit starting with $x(0) = 2$, while the second shows an orbit perturbed by a factor of 10^{-12}. The bottom subplot shows the pointwise differences $x(n) - y(n)$.

Figure 5 is a plot of the Lyapunov spectrum for this signal, with λ ranging from 1 to 5. For each value of λ, (3) is estimated using $m = 1000$, with an initial starting point of $x(0) = 2$. This spectrum is invariant in a basin of attraction, and so will only vary in different regions of stability. In the current case, the signal is entirely chaotic, and then undergoes periodic transitions from chaos to stability, as λ increases.

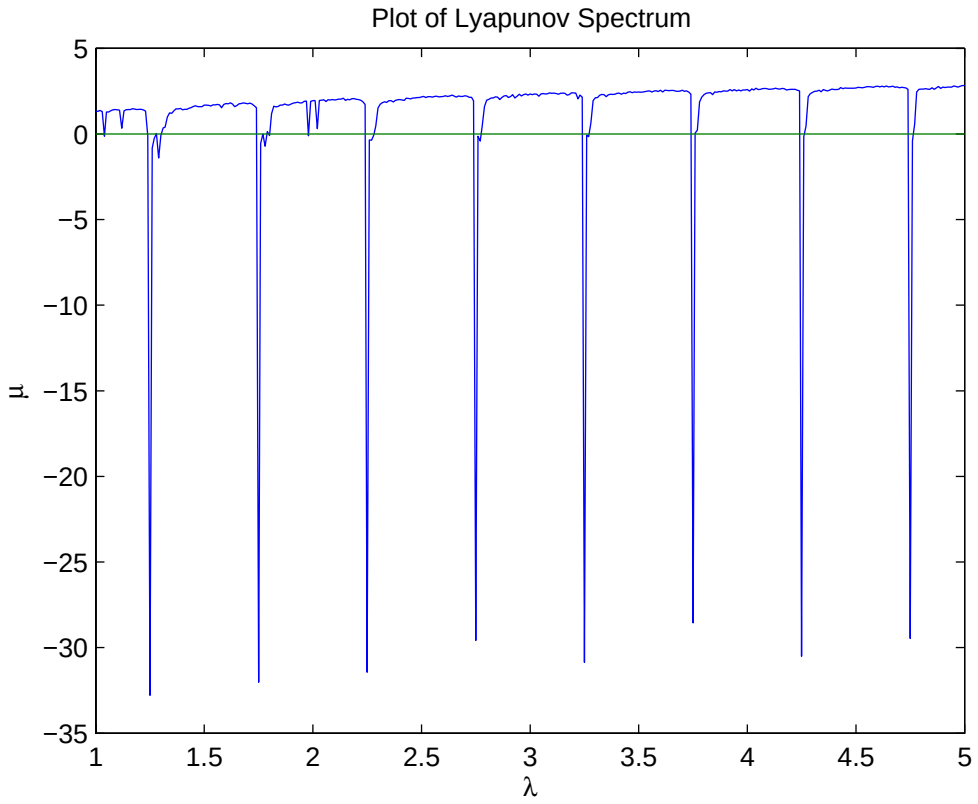

Figure 5: The Lyapunov spectrum for the signal with generator $\psi(x, \lambda) = \lambda \sin(2\pi x)$.

Figure 6 is a plot of the signal (2) as a function of λ. In the plot, λ ranges from 0.1 to 2, in increments of 0.001. The starting value for each iteration is $x(0) = 2$. For each λ, 10,000 iterations have been used to generate each point of the signal. The plot shows the stability of the solution as a function of λ, and then its transition to unstable and chaotic behaviour. An interesting feature of the transition to chaos is that the signal has a single stable solution, which evolves to a cone-like structure. A closer examination of the plot shows this behaviour occurs frequently.

Figure 7 contains a number of plots of the absolute value of the ambiguity function $\chi(\tau, \phi)$ for this signal, with $\lambda = 2$. Note that the signal under consideration is defined in terms of discrete time, and consequently the plot does not have the same resolution as those in Figures 2 and 3. The first two plots show the magnitude of the function, in (τ, ϕ) space, using colour-contour plots. The third plot shows the function $|\chi(\tau, \phi)|$ as a surface in space. The final plot shows the absolute value of the normalised autocorrelation function

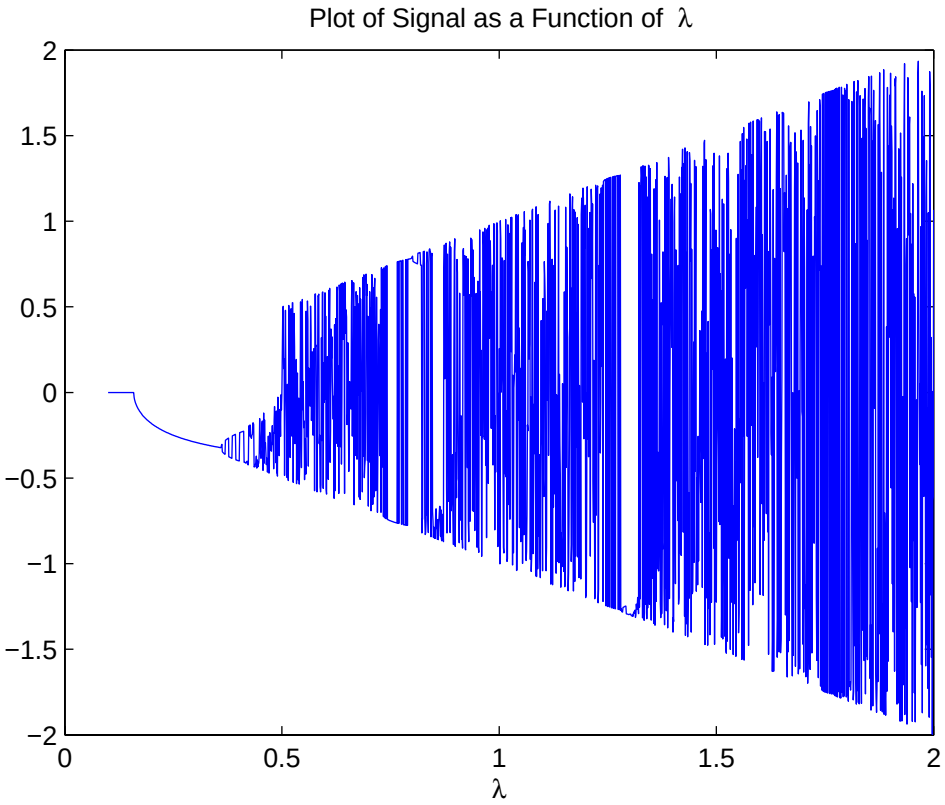

Figure 6: Evolution of iterations of the signal with generator $\psi(x,\lambda) = \lambda\sin(2\pi x)$, as a function of λ. For each λ, the vertical axis shows the result of 10,000 iterations of the signal.

$R(\tau) = \frac{1}{\max_\nu |\chi(\nu,0)|}\,|\chi(\tau,0)|$. The scale used for τ is discrete time units, while ϕ is in radians. The autocorrelation plot is over a larger range of values of τ in contrast to the three other plots. The ambiguity function in this case is almost a spike at the origin, with ripples of volume spread out from the origin $(\tau,\phi) = (0,0)$.

[Ringer, Frazer and Anderson 1999] class such signals as irregular or noise-like. Such signals are aperiodic and uncorrelated with themselves except on small intervals. The aperiodicity of the signal under consideration is inherently related to its chaotic nature. Figure 7 shows it has the expected autocorrelation property.

Due to the shape of the ambiguity functions in Figure 7, the corresponding signal should have an ability to resolve targets in both time delay and Doppler shift. However, it would be expected that such a signal may not provide a radar with a sufficient ability to differentiate targets in clutter with a low radar cross section (RCS), due to the extensive high sidelobe response in the ambiguity function.

Figure 8 shows the ambiguity function of Figure 7 on much larger time delay and Doppler shift intervals.

3.2 Example 2: $\psi(x, \lambda) = \sin(2\pi x) + \cos(2\pi\lambda x)$

The next example we consider is that with generator $\psi(x, \lambda) = \sin(2\pi x) + \cos(2\pi\lambda x)$. As for the first signal, we show its sensitivity to initial conditions. Figure 9 is a plot of the evolutions of two orbits of this signal, with one slighly perturbed, and corresponding pointwise differences of two evolutions of (2). The first begins with $x(0) = 0.01$, while the second is perturbed by 10^{-12}, so that it evolves from $y(0) = 0.01 + 10^{-12}$. In both cases we choose $\lambda = 4$. As can be observed from Figure 9, the two corresponding trajectories evolve together for a very short period, then diverge apart.

Next we examine the Lyapunov spectrum for this signal. Figure 10 is the Lyapunov spectrum, with λ ranging from 0.1 to 5. We have chosen the initial value $x(0) = 0.01$, for each λ, and $m = 1000$ as before. The spectrum shows this signal becomes increasingly more chaotic as λ increases. There is a very significant upward trend in Figure 10, and initial periods where there is stability.

Figure 11 is a plot of the signal, as a function of λ. In this case, λ varies from 0.1 to 2, in steps of 0.001. The initial condition is $x(0) = 0.01$, for each λ, and 10,000 iterations have been used to produce each value. The plot shows some very unusual behaviour. The Lyapunov spectrum over this range of λ shows the signal is chaotic, with short periods of stability. A close examination of Figure 11 shows that these periods of stability bifurcate to chaos in a conical structure. Near $\lambda = 0.5$ is a clear illustration of this. There is a short period where the signal has become stable, then bifurcates into a cone preceeding chaos. What is not so clear from the plot, but can be found on magnification, is that there are many of these cone-like transitions. One small one can be seen roughly after the significant cone, near $\lambda = 0.5$, becomes chaotic. At around $\lambda = 1.2$ another can be observed. Figure 12 is a magnification of the plot in Figure 11, over the region where $1.5 \leq \lambda \leq 1.7$. Increasing the number of iterations used, for each λ, improves the resolution of these plots and shows these transitions more clearly.

Figure 13 is a complementary plot of those in Figure 7, for this second signal under investigation. In this case we take $\lambda = 4$. As for the plots in Figure 7, we see that the absolute value of the ambiguity function is very similar to that of the first example. There is a difference in the contours as can be seen by comparing both second plots in Figures 7 and 13. As before, this signal is a member of the class of irregular/noise like signals. Its utility is exactly the same as that of the previous example.

Figure 14 is a complementary plot of that in Figure 8, showing the absolute value of the ambiguity function on a larger time delay and Doppler shift grid.

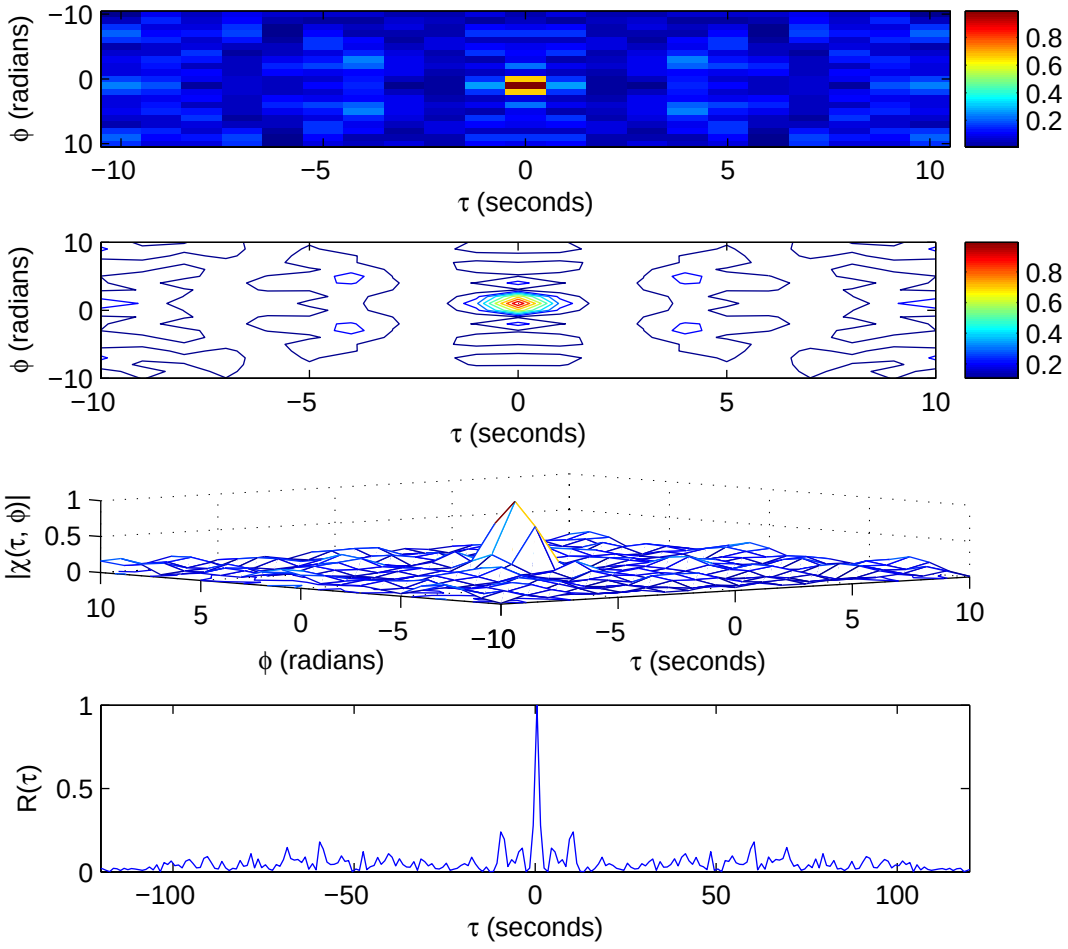

Figure 7: Ambiguity function and autocorrelation plots of the signal with generator as in Figure 6. We describe the plots from the top down. The first plot shows the absolute value of the ambiguity function's concentration in terms of a colour spectrum. The second plot shows a coloured contour version of the first. The third plot shows the absolute value of the ambiguity function as a surface in space. Finally, the fourth plot shows the normalised autocorrelation function. Since the corresponding signal is in discrete time, the time delay (τ) axis values are in discrete time units. Better graphical resolution is achieved by extending this axis (see Figure 8). The Doppler axis is in units of radians, while the time delay is measured in seconds. The absolute value of the ambiguity function is in a linear scale. The autocorrelation plot is shown over a larger spectrum of values of τ than used in the previous three subplots, and also is in a linear scale.

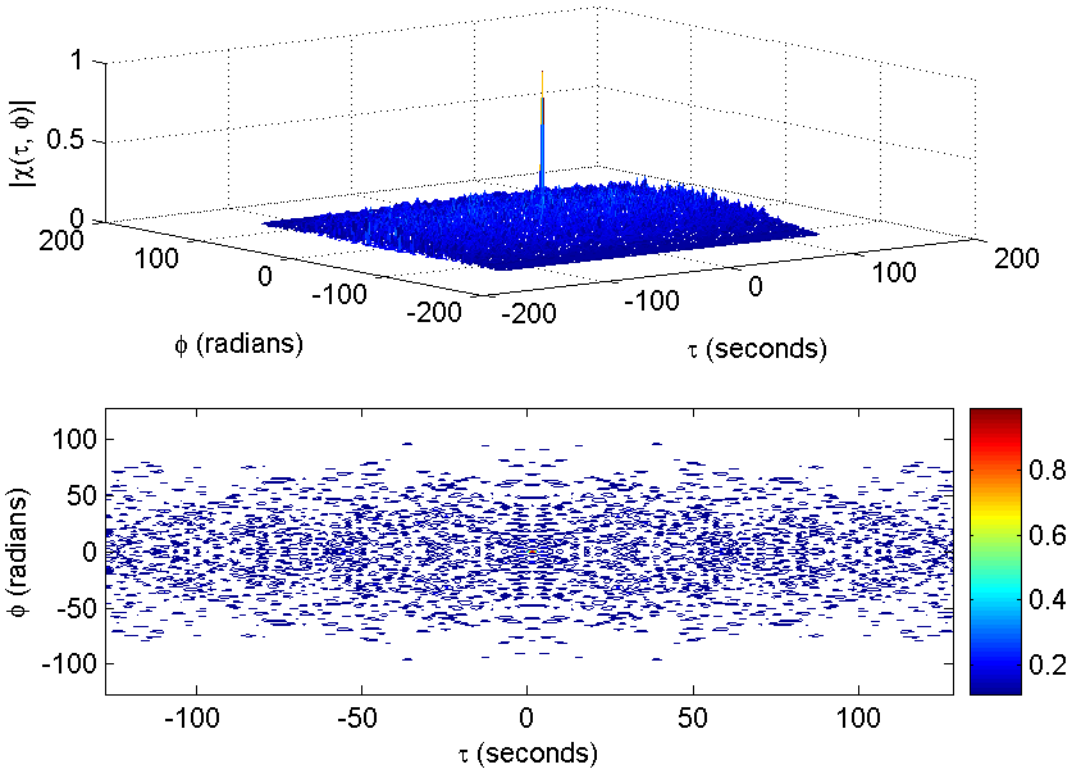

Figure 8: Ambiguity function plots for the signal with generator as in Figure 7, except the plots are over larger time delay and Doppler shift intervals. The top plot is of the absolute value of the ambiguity function, again as a surface, while the second plot shows the contours and corresponding ambiguity function values using a colourbar. The ambiguity function is in a linear scale.

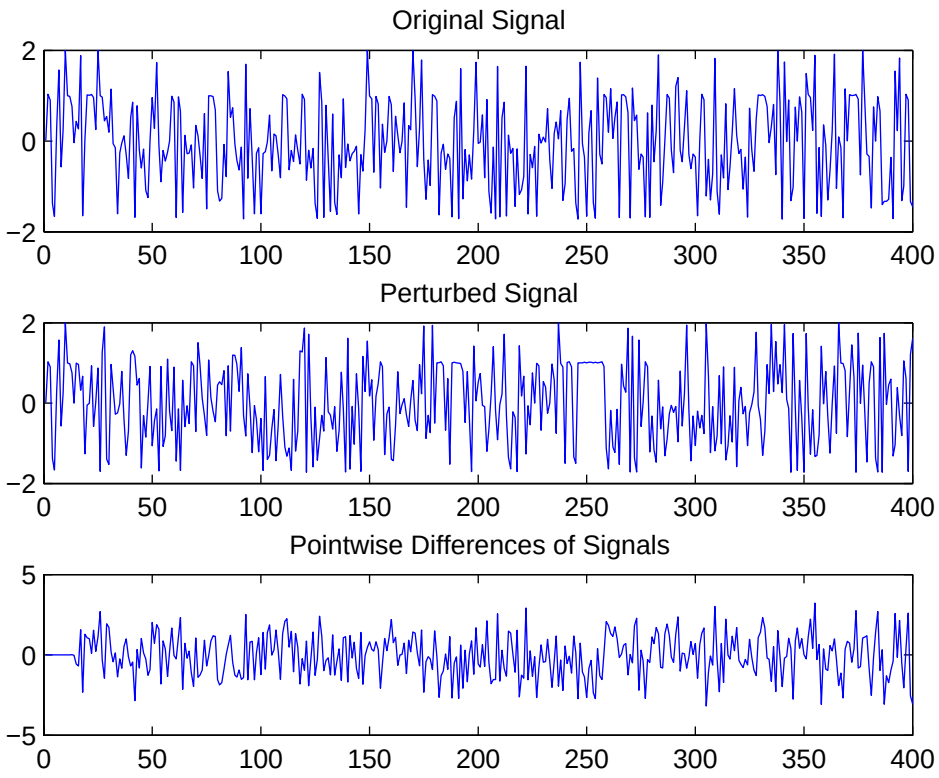

Figure 9: Differences of two signals generated with $\psi(x, \lambda) = \sin(2\pi x) + \cos(2\pi\lambda x)$*, with a perturbation of* 10^{-12} *in initial starting values. The top plot is of the original signal, the second is a slightly perturbed version, while the third is of the corresponding pointwise differences.*

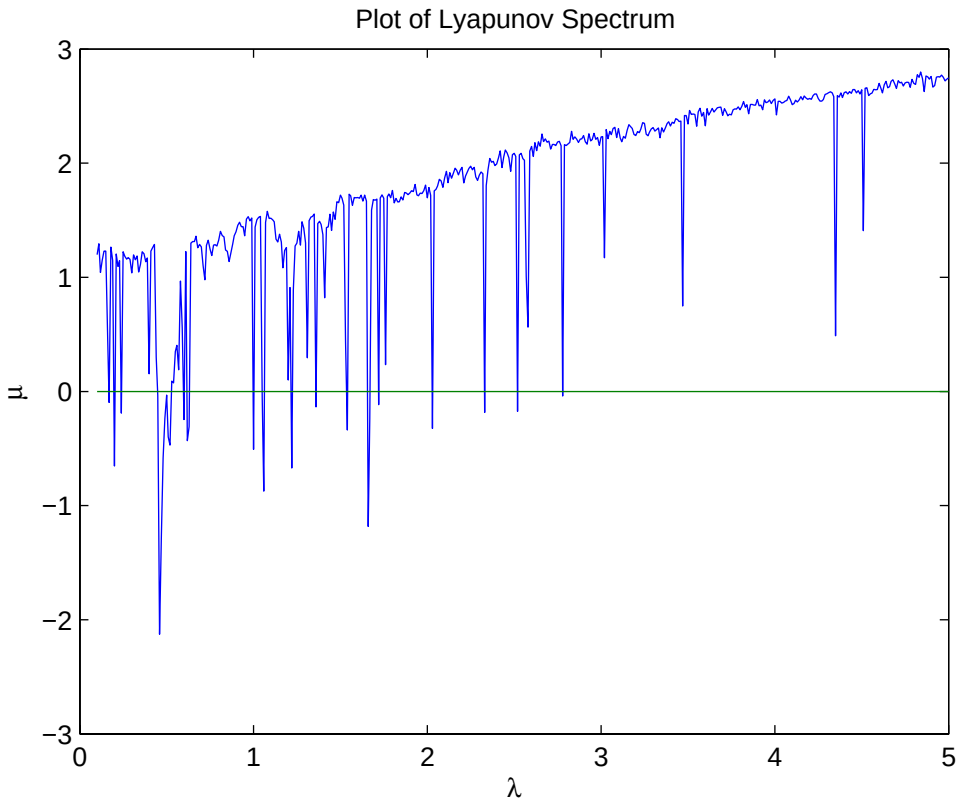

Figure 10: The Lyapunov spectrum for the signal with generator $\psi(x, \lambda) = \sin(2\pi x) + \cos(2\pi\lambda x)$.

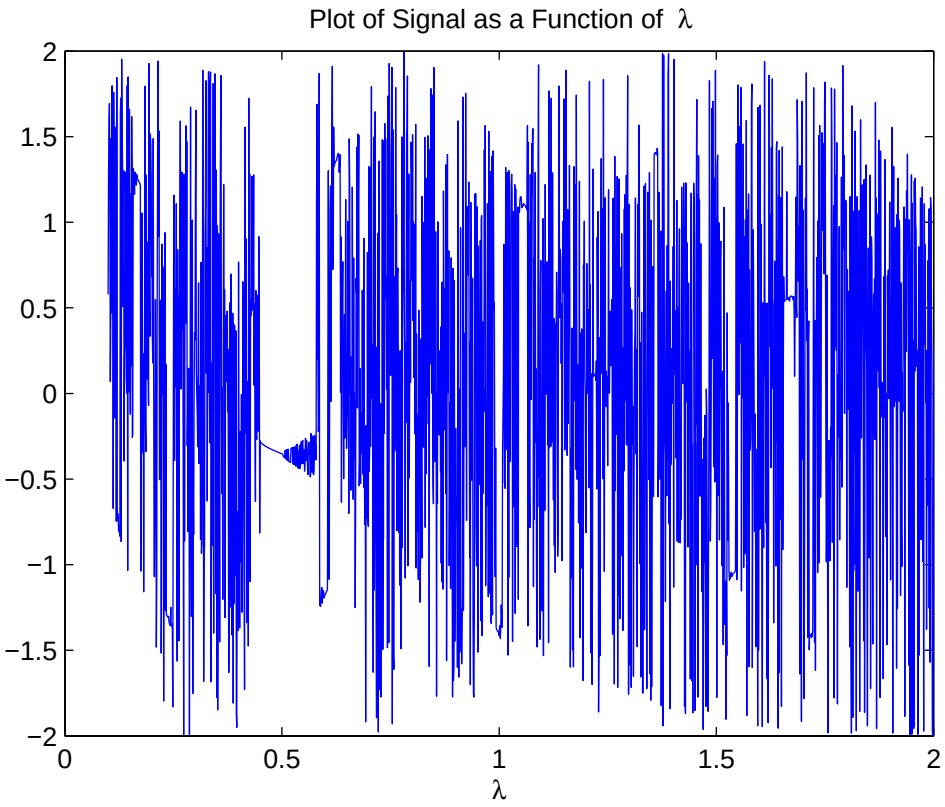

Figure 11: A plot of the result of 10,000 iterations of the signal with generator $\psi(x, \lambda) = \sin(2\pi x) + \cos(2\pi\lambda x)$*, as a function of* λ*.*

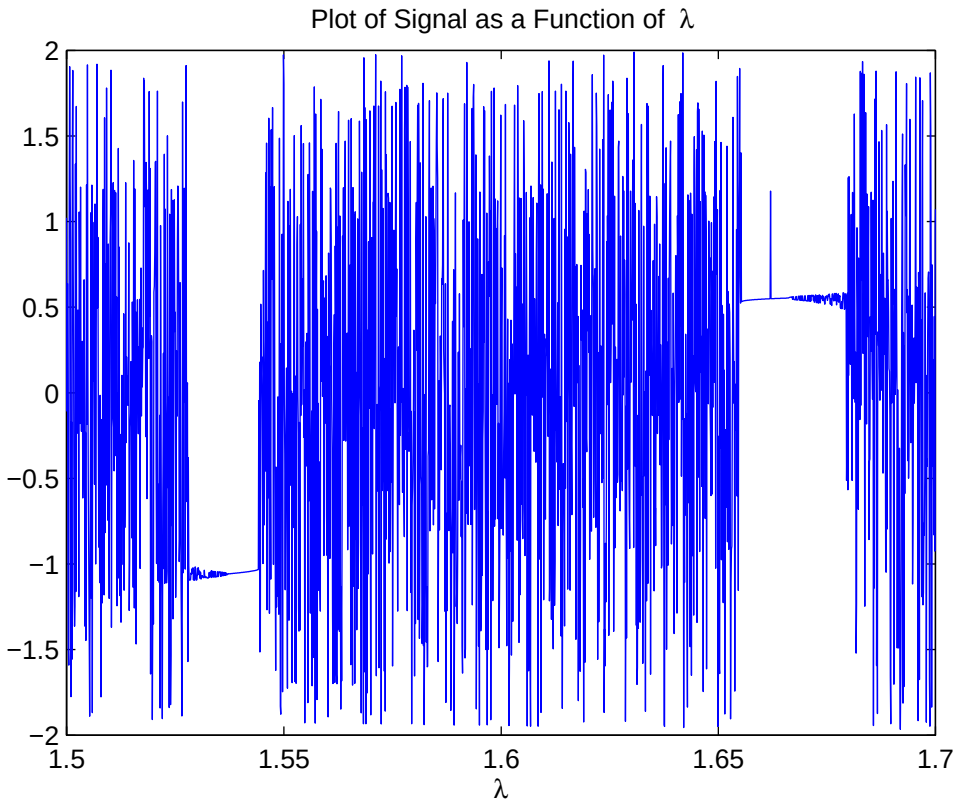

Figure 12: A magnification of the plot of Figure 11, with λ in the range from 1.5 to 1.7, in steps of 0.0001. The plot shows the generation of two new conical structures, indicating the transition from chaos to order. The first occurs at approximately $\lambda = 1.525$, while the second is at roughly $\lambda = 1.65$.

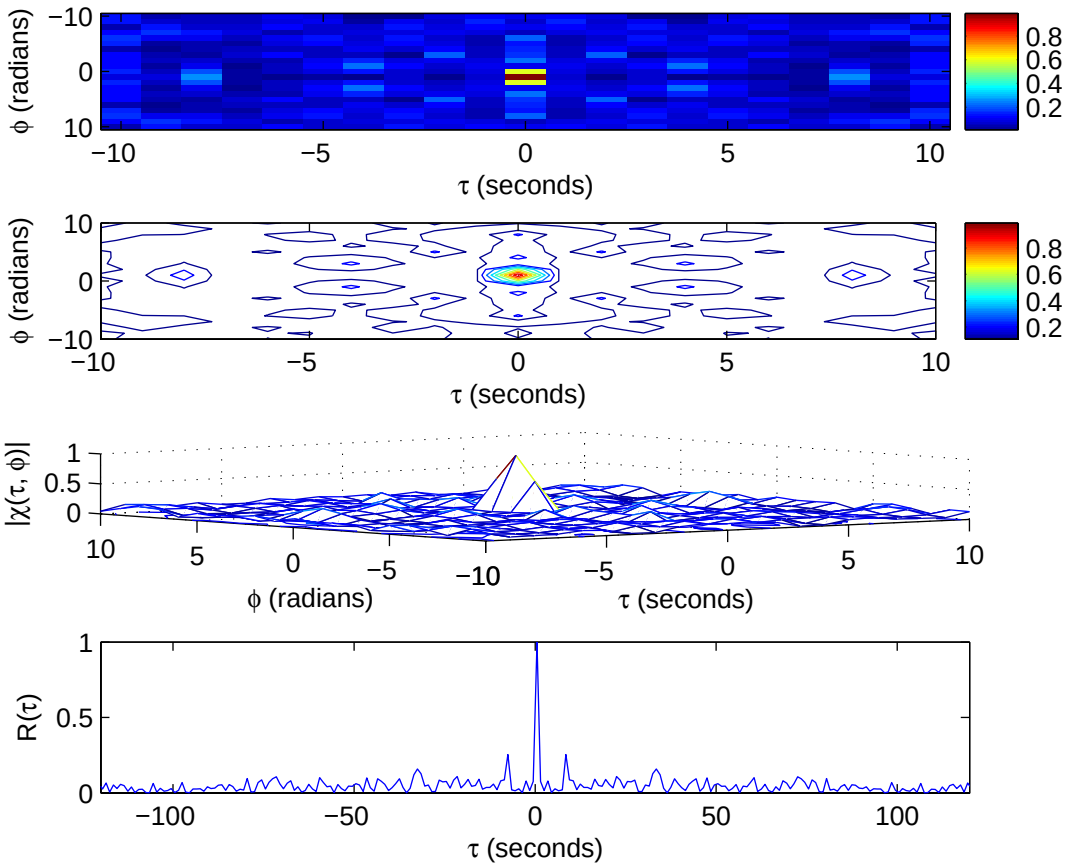

Figure 13: Ambiguity function plots for the signal with generator as for Figure 11. As in the ambiguity and autocorrelation plots in Figure 7 the first two subplots are colour-contour illustrations of the size of the absolute value of the ambiguity function in (τ, ϕ) space. The third plot is a surface plot, while the fourth plot is of the normalised autocorrelation function. The ambiguity function is in a linear scale.

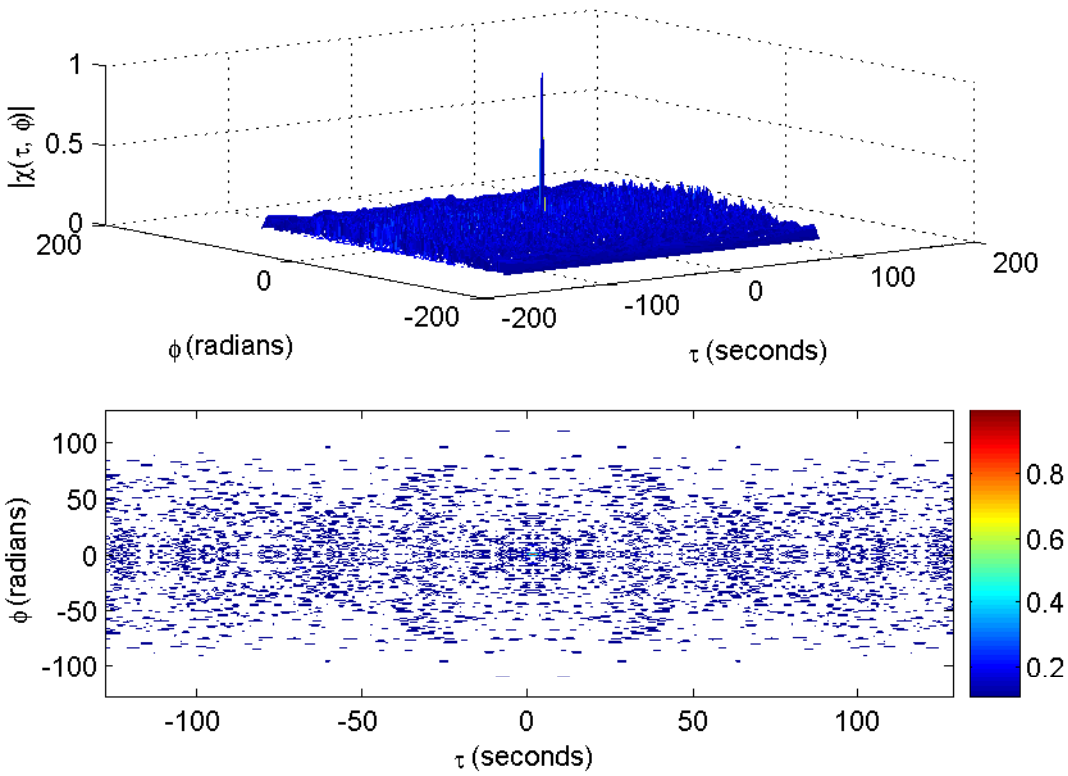

Figure 14: A plot similar to that of Figure 8, except for the signal of Figure 13. As before, the first plot shows the absolute value of the ambiguity function as a surface, while the second is a colour-coded contour plot. The ambiguity function is also in a linear scale, as previously.

4 Conclusions

This note introduced a class of recursively defined signals, motivated from [Haykin and Li 1995]. Their stability was analysed using a Lyapunov spectrum. These signals are members of a class of irreguar/noise like signals described in [Ringer, Frazer and Anderson 1999]. Based upon the shape of the absolute value of their ambiguity functions, we can conclude that they should have an ability to resolve targets in both time delay and Doppler shift. The disadvantage of such signals is that they have relatively high range and Doppler sidelobes in the ambiguity diagram, which will limit their ability to discriminate small targets against clutter, and small targets in the vicinity of larger targets.

5 Acknowledgements

Thanks are due to Dr Paul Berry for vetting the report, for comments provided by HRMA Dr Brett Haywood and to RLMR Dr Andrew Shaw for advice and suggestions related to the radar ambiguity function.

6 References

1. Benettin, G., Galgani, L., Giorgilli, A. and Strelcyn, J. (1980), Lyapunov characteristic exponents for smooth dynamical systems and for Hamiltonian systems; a method for computing all of them. Part I, II. Meccanica, **15**, 9–30.

2. Bird, G. J. A. (1974). *Radar Precision and Resolution.* (Pentch Press, London).

3. Cook, E. C. and Bernfield, M. (1967). *Radar Signals.* (Academic Press, New York).

4. Drazin, P. G. (1992). *Nonlinear Systems.* (Cambridge University Press, Cambridge).

5. Haykin, S. and Li, X. B. (1995), Detection of Signals in Chaos. IEEE Proc. **83**, 95-122.

6. Haykin, S. and Puthusserypady, S. (1999), *Chaotic Dynamics of Sea Clutter.* (Wiley, New York).

7. Hale, J. and Koçak, H. (1991), *Dynamics and Bifurcations.* (Springer-Verlag, New York).

8. Helstrom, C. W. (1960), *Statistical Theory of Signal Detection.* (Pergamon, London).

9. Levanon, N. (1988), *Radar Signals.* (Wiley, New York).

10. Levanon, N. and Mozeson, E. (2004), *Radar Signals.* (Wiley, New York).

11. Li, T. Y. and Yorke, J. A. (1975), Period Three Implies Chaos. Amer. Math. Monthly, **82**.

12. Lin, F-Y. and Liu, J-M. (2004), Diverse Waveform Generation Using Semiconductor Lasers for Radar and Microwave Applications. IEEE J. Quantum Elect. **40**, 682-689.

13. Lorenz, E. N. (1963), Deterministic nonperiodic flow. J. Atm. Science, **20**, 130–141.

14. Newhouse, S. (1984), Understanding chaotic dynamics. Chaos in Nonlinear Dynamical Systems, J. Chandra, Ed. SIAM.

15. Ringer, M. A., Frazer, G. J. and Anderson, S. J. (1999), Waveform Analysis of Transmitters of Opportunity for Passive Radar. DSTO–TR–0809.

16. Sobhy, M. I. and Shehata, A. R. (2000), Chaotic Radar Systems. Microwave Symp. Digest, IEEE MTT-S **3**, 1701-1704.

17. Strogatz, S. (1994), *Nonlinear Dynamics and Chaos.* (Addison-Wesley, Massachusetts).

18. Williams, G. P. (1997), *Chaos Theory Tamed.* (Taylor and Francis, London).

19. Wolf, A. (1986), *Quantifying chaos with Lyapunov Exponents.* (in *Chaos*, A. V. Holden Ed., Princeton University Press, Princeton, New Jersey.

20. Wu, X., Liu, W., Zhao, L. and Fu, J. (2001), Chaotic Phase Code for Radar Pulse Compression. Proceed. IEEE Radar Conf. 2001, 279-283.

21. Zigangirov, K. S. (2004), *Theory of Code Division Multiple Access Communication.* (IEEE Series on Digital & Mobile Communication, Wiley-IEEE Press).

DISTRIBUTION LIST

Examples of a Class of Chaotic Radar Signals

Graham V. Weinberg and Aris Alexopoulos

AUSTRALIA

	No. of copies
DEFENCE ORGANISATION	
Task Sponsor	
Director General Maritime Development	1
S&T Program	
Chief Defence Scientist Deputy Chief Defence Scientist (Policy) AS Science Corporate Management Director General Science Policy Development	1 Shared copy
Counsellor, Defence Science, London	Doc Data Sheet
Counsellor, Defence Science, Washington	Doc Data Sheet
Scientific Adviser to MRDC, Thailand	Doc Data Sheet
Scientific Adviser Joint	1 (pdf format)
Navy Scientific Adviser	1 (pdf format)
Scientific Adviser, Army	Doc Data Sheet
Air Force Scientific Adviser	Doc Data Sheet
Scientific Adviser to the DMO	Doc Data Sheet
Systems Sciences Laboratory	
EWSTIS	1 (pdf format)
Chief, Electronic Warfare and Radar Division, Dr Len Sciacca	Doc Data Sheet & Dist List
Research Leader, Microwave Radar, Dr Andrew Shaw	Doc Data Sheet & Dist List
Task Manager and Head, Radar Modelling and Analysis Group, Dr Brett Haywood	1 (pdf format)
Author, Dr Graham V Weinberg, EWRD	10
Author, Dr Aris Alexopoulos, EWRD	10
Dr Paul Berry, EWRD	1 (pdf format)
Dr Anthony Szabo, WSD	1 (pdf format)
DSTO Library and Archives	
Library, Edinburgh	1
Defence Archives	1 (pdf format)

Capability Development Group	
Director General Capability and Plans	Doc Data Sheet
Assistant Secretary Investment Analysis	Doc Data Sheet
Director Capability Plans and Programming	Doc Data Sheet
Chief Information Officer Group	
Director General Australian Defence Simulation Office	Doc Data Sheet
AS Information Strategies and Futures	Doc Data Sheet
Director General Information Services	Doc Data Sheet
Strategy Group	
Director General Military Strategy	Doc Data Sheet
Assistant Secretary Strategic Policy	Doc Data Sheet
Assistant Secretary Governance and Counter-Proliferation	Doc Data Sheet
Navy	
Maritime Operational Analysis Centre, Building 89/90 Garden Island Sydney NSW Deputy Director (Operations) and Deputy Director (Analysis)	Doc Data Sheet & Dist List
Director General Navy Capability, Performance and Plans, Navy Headquarters	Doc Data Sheet
Director General Navy Strategic Policy and Futures, Navy Headquarters	Doc Data Sheet
Air Force	
SO (Science), Headquarters Air Combat Group, RAAF Base, Williamtown NSW 2314	Doc Data Sheet & Exec Summ
Army	
ABCA National Standardisation Officer, Land Warfare Development Sector, Puckapunyal	Doc Data Sheet e-mailed
SO (Science), Land Headquarters (LHQ), Victoria Barracks, NSW	Doc Data Sheet & Exec Summ
SO (Science), Deployable Joint Force Headquarters (DJFHQ)(L), Enoggera QLD	Doc Data Sheet
Joint Operations Command	
Director General Joint Operations	Doc Data Sheet
Chief of Staff Headquarters Joint Operations Command	Doc Data Sheet
Commandant ADF Warfare Centre	Doc Data Sheet
Director General Strategic Logistics	Doc Data Sheet
COS, Australian Defence College	Doc Data Sheet
Intelligence and Security Group	
AS, Concepts, Capability and Resources	1 (pdf format)

DGSTA, Defence Intelligence Organisation	1
Director, Advanced Capabilities	Doc Data Sheet
Manager, Information Centre, Defence Intelligence Organisation	1 (pdf format)

Defence Materiel Organisation

Deputy CEO	Doc Data Sheet
Head Aerospace Systems Division	Doc Data Sheet
Head Maritime Systems Division	Doc Data Sheet
Head, Electronic and Weapon Systems Division	Doc Data Sheet
Program Manager Air Warfare Destroyer	Doc Data Sheet
CDR Joint Logistics Command	Doc Data Sheet

OTHER ORGANISATIONS

National Library of Australia	1 (pdf format)
NASA (Canberra)	1 (pdf format)

UNIVERSITIES AND COLLEGES

Australian Defence Force Academy

Library	1 (pdf format)
Head of Aerospace and Mechanical Engineering	1 (pdf format)
Serials Section (M List), Deakin University Library, Geelong, Vic	1 (pdf format)
Hargrave Library, Monash University	Doc Data Sheet (pdf format)

OUTSIDE AUSTRALIA

INTERNATIONAL DEFENCE INFORMATION CENTRES

US Defense Technical Information Center	1	(pdf format)
UK Dstl Knowledge Services	1	(pdf format)
Canada Defence Research Directorate R&D Knowledge & Information Management (DRDKIM)	1	(pdf format)
NZ Defence Information Centre	1	(pdf format)

ABSTRACTING AND INFORMATION ORGANISATIONS

Library, Chemical Abstracts Reference Service	1	(pdf format)
Engineering Societies Library, US	1	(pdf format)
Materials Information, Cambridge Scientific Abstracts, US	1	(pdf format)
Documents Librarian, The Center for Research Libraries, US	1	(pdf format)

SPARES

DSTO Edinburgh Library	5

Total number of copies:	**Printed**	**29**
	PDF	**22**

DEFENCE SCIENCE AND TECHNOLOGY ORGANISATION DOCUMENT CONTROL DATA				1. CAVEAT/PRIVACY MARKING
2. TITLE Examples of a Class of Chaotic Radar Signals			3. SECURITY CLASSIFICATION Document (U) Title (U) Abstract (U)	
4. AUTHORS Graham V. Weinberg and Aris Alexopoulos			5. CORPORATE AUTHOR Defence Science and Technology Organisation PO Box 1500 Edinburgh, South Australia, Australia 5111	
6a. DSTO NUMBER DSTO–TN–0660	6b. AR NUMBER AR-013-488		6c. TYPE OF REPORT Technical Note	7. DOCUMENT DATE August, 2005
8. FILE NUMBER 2005/1043045/1	9. TASK NUMBER NAV 01/299	10. SPONSOR DGMD	11. No OF PAGES 22	12. No OF REFS 21
13. URL OF ELECTRONIC VERSION http://www.dsto.defence.gov.au/corporate/reports/DSTO–TN–0660.pdf			14. RELEASE AUTHORITY Chief, Electronic Warfare and Radar Division	
15. SECONDARY RELEASE STATEMENT OF THIS DOCUMENT *Approved For Public Release* OVERSEAS ENQUIRIES OUTSIDE STATED LIMITATIONS SHOULD BE REFERRED THROUGH DOCUMENT EXCHANGE, PO BOX 1500, EDINBURGH, SOUTH AUSTRALIA 5111				
16. DELIBERATE ANNOUNCEMENT No Limitations				
17. CITATION IN OTHER DOCUMENTS No Limitations				
18. DEFTEST DESCRIPTORS Radar signals, Target acquisition, Chaos theory				
19. ABSTRACT This note is a preliminary study of radar signals viewed as discretised nonlinear dynamical systems. Motivated by [Haykin and Li 1995], a class of recursively defined signals is introduced, and two specific examples are considered. It will be shown that such signals can exhibit complex dynamics in phase space. This means that they experience sensitive dependence on initial conditions. Using the Lyapunov spectrum, we determine the stability of these signals. We will also investigate whether such signals are of practical use in radar by examining their ambiguity functions.				